0026-895X/96/051057-08$3.00/0

MOLECULAR PHARMACOLOGY, 50:1057–1064 (1996).

Differences in the Inhibition of Human Immunodeficiency Virus Type 1 Reverse Transcriptase DNA Polymerase Activity by Analogs of Nevirapine and [2′,5′-bis-*o*-(*tert*-Butyldimethylsilyl)-3′-spiro-5″-(4″-amino-1″, 2″-oxathiole-2″,2″-dioxide] (TSAO)

DOMINIQUE ARION, RONALD S. FLETCHER, GADI BORKOW, MARÍA-JOSÉ CAMARASA, JAN BALZARINI, GARY I. DMITRIENKO, and MICHAEL A. PARNIAK

Lady Davis Institute for Medical Research and McGill University AIDS Centre, Sir Mortimer B. Davis Jewish General Hospital, Montreal, Quebec H3T 1E2 Canada (D.A., R.S.F., G.B., M.A.P.), Instituto de Quimica Médica, Consejo Superior de Investigaciones Cientificas, Madrid E-28006, Spain (M.-J.C.), Rega Institute for Medical Research, Katholieke Universiteit Leuven, B-3000 Leuven, Belgium (J.B.) and Department of Chemistry, University of Waterloo, Waterloo, Ontario N2L 3G1 Canada (G.I.D.)

Received March 27, 1996; Accepted July 17, 1996

SUMMARY

We compared the inhibition of HIV-1 reverse transcriptase (RT) by 1-[2′,5′-bis-O-(t-butyldimethylsilyl)-β-D-ribofuranosyl]-3′-spiro-5″-(4″-amino-1″, 2″-oxathiole-2″,2″-dioxide)-3-ethylthymine (TSAOe^{3}T) and the nonnucleoside RT inhibitor (NNRTI) 9-aminonevirapine (9-NH_2N). Both compounds were equally effective against p51/p66 heterodimeric RT RNA-dependent DNA polymerase activity, although TSAOe^{3}T was a much better inhibitor of the p51/p51 and p66/p66 RT homodimers. Inhibition by TSAOe^{3}T and 9-NH_2N combinations was essentially additive. TSAOe^{3}T did not protect either free RT or the RT-template/primer-deoxynucleoside triphosphate ternary complex from irreversible inactivation by the photolabel 9-azidonevirapine. Slight protection of the RT-template/primer binary complex was noted, but only at high TSAOe^{3}T/photolabel ratios. Analysis of RT polymerization product profiles under both continuous- and single-processive cycle conditions showed that 9-NH_2N prevented the formation of full-length product with a corresponding accumulation of smaller polymerization products. In contrast, all products formed in the absence of inhibitor, including full-length product, were noted in TSAOe^{3}T-inhibited reactions, albeit at reduced levels. TSAOe^{3}T thus inhibits HIV-1 RT by a different mechanism than NNRTI such as nevirapine. Our data suggest that TSAOe^{3}T and 9-NH_2N interact differently with HIV-1 RT, perhaps by binding to distinct sites on the enzyme.

RT is an essential enzyme for the replication of HIV-1, the primary causative agent of acquired immune deficiency syndrome. HIV-1 RT is virus-specific and multifunctional; it exhibits RDDP, DDDP and RNase H activities. This enzyme thus represents an attractive target for the development of potential anti-HIV chemotherapeutics. Substantial effort on the part of investigators in academia and in the pharmaceutical industry has resulted in the identification of a number of RT inhibitors, most of which can be grouped into two major classes.

The first class consists of the dideoxy analogs of the dNTP substrates; it includes such compounds as AZT, 2′,3′-dideoxyinosine, 2′,3′-dideoxycytidine, 2′,3′-didehydro-2′,3′-dideoxythymidine, and 2′,3′-dideoxy-3′-thiacytidine (1–5). These dideoxynucleoside compounds are competitive inhibitors with respect to the dNTP substrates and also inhibit RT by acting as chain terminators during DNA polymerization (6). Recent studies indicate that chain termination is likely to be the primary mechanism of inhibition by dideoxynucleoside inhibitors (7, 8).

The second major class consists of the NNRTIs; it includes such compounds as nevirapine (9, 10), tetrahydroimidazo[4,5,1-*jk*][1,4]-benzodiazepine-2(1*H*)-thione (11), the pyridinones (12), and the carboxanilides (13–15). The NNRTIs function by interacting with a site on the p66 subunit of RT

This work was supported in part by Grant MRC PG-11899 from the Medical Research Council of Canada to M.A.P.

ABBREVIATIONS: RT, reverse transcriptase; HIV-1, human immunodeficiency virus type 1; dNTP, deoxynucleoside triphosphate; 9-AN, 9-azido-5,6-dihydro-11-ethyl-6-methyl-11H-pyrido[2,3-*b*][1,5]benzodiazepin-5-one; 9-NH_2N, 9-amino-5,6-dihydro-11-ethyl-6-methyl-11H-pyrido[2,3-*b*][1,5]benzodiazepin-5-one; AZT, 3′-azido-3′-deoxythymidine; DDDP, DNA-dependent DNA polymerase; NNRTI, nonnucleoside reverse transcriptase inhibitor; PAGE, polyacrylamide gel electrophoresis; RDDP, RNA-dependent DNA polymerase; TCA, trichloroacetic acid; T/P, template/primer; TSAO, 2′,5′-bis-O-(*tert*-butyldimethylsilyl)-3′-spiro-5″-(4″-amino-1″,2″-oxathiole-2″,2″-dioxide); TSAOe^{3}T, 1-[2′,5′-bis-O-(*tert*-butyldimethylsilyl)-β-D-ribofuranosyl]-3′-spiro-5″-(4″-amino-1″,2″-oxathiole-2″,2″-dioxide)-3-ethylthymine; DMSO, dimethylsulfoxide.

that is near but distinct from the catalytic site (9, 10, 16–20). However, the mechanism by which NNRTIs inhibit RT DNA polymerase activity is not yet clear.

In addition to these two major classes of RT inhibitors, there are other anti-RT agents that are not readily classified, such as TSAO and its derivatives (21, 22). Although TSAO inhibitors are nucleoside-based, they are highly modified and exhibit inhibition kinetics characteristic of NNRTI (21). HIV-1 resistance to TSAO derivatives correlates with a unique mutation [E138K (23)] not normally noted with resistance to most NNRTI or to dideoxynucleoside inhibitors. Interestingly, resistance to TSAO is attributable to alteration of the p51 subunit of the p51/p66 RT heterodimer (24, 25), the apparently "inactive" subunit of the p51/p66 RT heterodimer. Crystallographic studies have shown that the E138 residue of p51 can contribute to the NNRTI binding pocket of the p51/p66 RT heterodimer (18–20).

In this study, we compared the inhibition of RT by analogs of TSAO and the NNRTI nevirapine to determine whether these structurally different RT inhibitors function in a similar manner and whether they bind to the same site on HIV-1 RT. Our data show that TSAO and nevirapine analogs lead to very different inhibition profiles, which implies that these classes of inhibitors bind differently to HIV-1 RT, perhaps by interacting with different sites on the enzyme.

Materials and Methods

The photoactivatable nevirapine analog 9-AN was synthesized as described previously (26). The nevirapine analog inhibitor 9-NH_2N was obtained as an intermediate in the synthesis of 9-AN. ^{1}H NMR and elemental analyses of 9-AN and 9-NH_2N were entirely consistent with the chemical structures (Fig. 1). Both 9-AN and 9-NH_2N inhibit HIV-1 RT with a potency similar to that of nevirapine, and both compounds have been shown to bind to the same site on RT as nevirapine (27). The ethyl derivative of TSAO, TSAOe^{3}T (Fig. 1), is one of the most potent of the TSAO analogs and was prepared as described previously (28).

[^{3}H]deoxy-TTP and [^{3}H]deoxy-GTP were purchased from New England Nuclear-Dupont (Boston, MA). [α-^{32}P]dNTPs were from Amersham (Mississauga, ON). The homopolymeric T/P poly(rC)-oligo(dG)$_{12-18}$, poly(rA)-oligo(dT)$_{12-18}$, and poly(dC)-oligo(dG)$_{12-18}$ were obtained from Pharmacia (Montreal, Quebec, Canada). The heteropolymeric DDDP T/P, calf thymus-activated DNA, was a product of Sigma (St. Louis, MO). Heteropolymeric RDDP T/P was prepared using the T7 polymerase RNA transcript from plasmid pHIV-PBS and a synthetic 18-mer oligonucleotide primer as described previously (7, 29). Recombinant heterodimeric p51/p66 and homodimeric p51/p51 and p66/p66 forms of HIV-1 RT were purified from lysates of *Escherichia coli* JM-105 transformed with expression plasmids pRT66 and pRT51 (7) using a rapid single-step purification method we have devised (30). All other reagents were of the highest quality available and were used without further purification.

Assay of RT RDDP and DDDP activities. HIV-1 RT DNA polymerase activity was determined with a fixed-time assay. Briefly, reaction mixtures (50–100 μl total volume) contained 50 mM Tris·HCl, pH 7.8, 37°, 60 mM KCl, 10 mM $MgCl_2$, 5 mM dithiothreitol, 5 nM p51/p66 RT, variable template/primer (generally 150 nM), and 0.5–25 μM of ^{3}H- or ^{32}P-labeled dNTP substrate. Aliquots of inhibitor stock solutions in DMSO were added such that the final DMSO concentration never exceeded 2%. Neither RT RDDP nor DDDP activity was affected by this concentration of DMSO (14). Reaction assays were incubated at 37°, then quenched with 500 μl of cold 20 mM sodium pyrophosphate in 10% TCA. After 15 min on ice, the samples were filtered on Whatman 934-AH glass fiber filters (Fisher Scientific, Montreal, Quebec, Canada), washed with 10% TCA and 95% ethanol, and analyzed by liquid scintillation counting.

The ability of TSAOe^{3}T to protect the various mechanistic forms of RT from irreversible inactivation by the photolabeled 9-AN was assessed exactly as described for the carboxanilide NNRTI (14). Briefly, RT (0.4 μM) in 40 μl of 50 mM Tris·HCl, pH 8.0, 25°, was incubated with 9-AN photolabel (1 μM) in the absence or presence of TSAOe^{3}T (12.5 μM) or 9-NH_2N (12.5 μM) and illuminated at 365 nm at an intensity of 20 μW/cm^2. At various times, aliquots were withdrawn and diluted 800-fold into reaction assays for the determination of residual RT activity. In experiments concerning inactivation of the RT-T/P binary complex, RT was preincubated with 15 μg/ml poly(rC)-oligo(dG)$_{12-18}$ for 10 min before the inhibitors and the 9-AN were added and irradiation was performed as above. In experiments concerning inactivation of the RT-T/P-dNTP ternary complex, RT was first preincubated with 15 μg/ml poly(rC)-oligo(dG)$_{12-18}$ for 10 min, and then dGTP (10 μM final concentration), the inhibitors and 9-AN were added sequentially before irradiation.

Inhibition of RT DNA polymerase activity by combinations of TSAOe^{3}T and 9-NH_2N was assessed by calculation of the combination index (31), as we have described previously (15). Combination indices of less than 1 indicate synergistic inhibition, whereas values equal to or more than 1 imply additive and antagonistic inhibition, respectively.

PAGE analysis of RT inhibition products. Unless otherwise indicated, experiments were carried out in 100 μl total volume using conditions similar to that described above for assay of RT polymerase. After incubation at 37°, a portion of the reaction mixture was removed and added to 500 μl of 10% TCA/20 mM sodium pyrophosphate for determination of total RT polymerase activity. The remainder of the reaction assay was immediately placed on ice; then the reaction products were isolated by extraction with phenol/chloroform, precipitation with sodium acetate/ethanol, and centrifugation

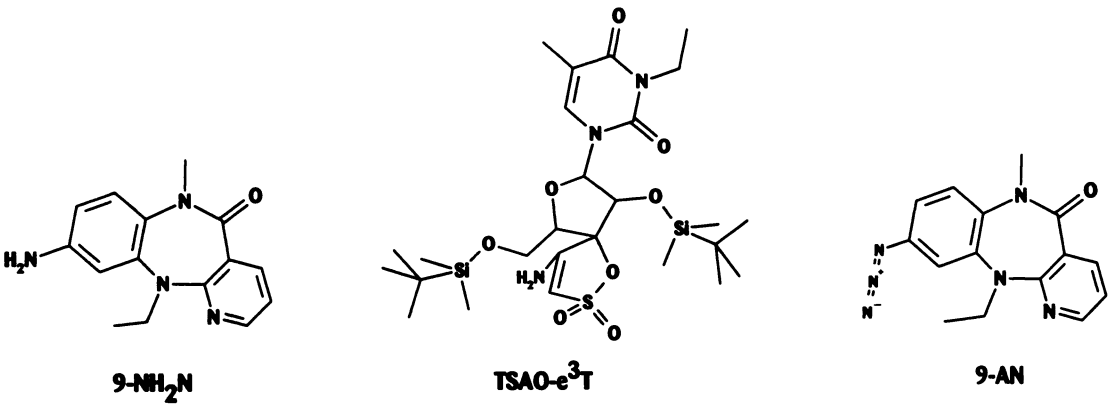

Fig. 1. Structures of the inhibitors used in these studies.

at 12,000 × *g* for 10 min. The reaction products were dissolved in 25 μl of Tris/Borate/EDTA buffer (1× = 45 mM Tris/borate and 1 mM EDTA, pH 8.0) containing 98% deionized formamide, 10 mM EDTA, 1 mg/ml bromphenol blue and 1 mg/ml xylene cyanol, heated at 100° for 5 min, then analyzed by denaturing PAGE followed by autoradiography (Kodak X-OMAT film). The size of the polymerization products is designated as n + *x*, where n is the 18-nucleotide primer and *x* is the number of nucleotides by which the primer has been elongated.

Processivity analysis of RT polymerization. These studies used heparin (1 mg/ml final concentration). Heparin competes with the T/P for binding to free RT (32). This allows observation of the polymerization product distribution under conditions of a single processive cycle, because RT, upon dissociation from the T/P, is trapped by the heparin and therefore unable to rebind to the T/P and continue transcription of the partial polymerization products. In these experiments, RT and T/P were preincubated in 50 mM Tris·HCl pH 7.8, 37°, 60 mM KCl, and 10 mM dithiothreitol for 5 min before starting the reaction by addition of dNTPs/$MgCl_2$ and heparin in the absence or presence of inhibitor. The effectiveness of the trap was confirmed by preincubating RT with heparin for 5 min before addition of the T/P. Under these conditions, less than 2% RT activity was noted (data not shown). No detectable bands were noted on autoradiographic analysis, even after 6 days of exposure.

Results

Effect of T/P identity on inhibition of RT RDDP and DDDP activities by 9-NH_2N and TSAOe^{3}T. The apparent effect of NNRTI on RT DNA polymerase activity depends in part on the T/P used in the *in vitro* assay (15, 21). To establish appropriate conditions for our product distribution analyses, we studied the ability of 9-NH_2N and TSAOe^{3}T to inhibit RT-catalyzed DNA polymerization using a variety of T/P (Table 1). Both TSAOe^{3}T and 9-NH_2N showed essentially similar inhibitory activity with all T/P, except for activated calf thymus DNA. With the latter T/P, TSAOe^{3}T was significantly more effective than 9-NH_2N.

Inhibition of DNA polymerase activity of the multiple forms of RT by TSAOe^{3}T and 9-NH_2N. Resistance to nevirapine correlates with mutations in the p66 subunit of RT (33), whereas resistance to TSAO is caused by a mutation in the p51 subunit of the enzyme (24, 25). Our purification protocol (30) enables isolation of active p51/p51, p66/p66, and p51/p66 forms of recombinant HIV-1 RT. We found that TSAOe^{3}T and 9-NH_2N had similar inhibitory potency against the p51/p66 RT heterodimer (Table 2). However, compared with 9-NH_2N, TSAOe^{3}T was a much better inhibitor of both the RDDP and DDDP activities of the p66 and p51 homodimeric forms of RT (Table 2). Indeed, 9-NH_2N was entirely inactive against p51 RT DDDP activity, whereas TSAOe^{3}T showed good inhibition (Table 2).

TABLE 1

Effect of T/P on inhibition of HIV-1 p51/p66 RT by TSAOe^{3}T and 9-NH_2N.

Values are the averages of determinations from two separate experiments.

Template/primer	IC_{50}	
	TSAOe^{3}T	9-NH_2N
	μM	
RDDP		
Poly (rA)-oligo (dT)	2.5	1.0
Poly (rC)-oligo (dG)	0.7	0.5
Heteropolymeric	1.0	0.3
DDDP		
Poly (dC)-oligo (dG)	1.3	0.4
Heteropolymeric	1.0	6.5

TABLE 2

Inhibition of HIV-1 RT multiple forms by TSAOe^{3}T and 9-NH_2N.

The values are averages of two separate experiments. RDDP and DDDP assays were carried out with poly (rC)-oligo (dG) and poly (dC)-oligo (dG) respectively, as described in Materials and Methods.

RT form	IC_{50}			
	RDDP		DDDP	
	TSAOe^{3}T	9-NH_2N	TSAOe^{3}T	9-NH_2N
	μM			
p51/p66	0.7	0.5	1.3	0.4
p66/p66	0.2	1.7	0.8	8[a]
p51/p51	[b]	[b]	5.5	>25[c]

[a] A maximum of 50% inhibition was attained. The value reported is that at which 50% inhibition was noted.
[b] Essentially no RDDP activity was noted with p51 RT.
[c] RT DDDP activity was equivalent to no drug controls at an inhibitor concentration of 25 μM.

Effect of TSAOe^{3}T and 9-NH_2N combinations on inhibition of RT RDDP activity. Analysis of enzyme inhibition by combinations of inhibitors compared with that by each inhibitor alone can provide information concerning the mode of binding of these inhibitors (31). We have shown that analysis of the effect of drug combinations on HIV-1 RT requires characterization of inhibition of each of the mechanistic forms of the enzyme, namely free RT, RT-T/P binary complex, and the RT-T/P-dNTP ternary complex (14, 15). The level of these RT mechanistic forms in reaction assays can be varied by alteration of T/P and dNTP concentrations. Inhibition of RT RDDP activity by combinations of TSAOe^{3}T and 9-NH_2N was essentially additive in assays that contained primarily the RT-T/P binary complex or the RT-T/P-dNTP ternary complex (Table 3: assay conditions B and C, respectively). Interestingly, inhibition of assays that contained free RT seemed to be partially antagonistic (Table 3; assay condition A).

Photoprotection analysis of the binding of TSAOe^{3}T and 9-NH_2N to RT. We studied the ability of TSAOe^{3}T and 9-NH_2N to protect RT from irreversible inactivation by the photoactivatable nevirapine analog 9-AN using techniques similar to those employed in our studies of the carboxanilide NNRTI (14). Control studies carried out in the dark (i.e., without irreversible inactivation) showed that 9-AN and TSAOe^{3}T were comparable inhibitors of RT RDDP activity (data not shown).

TABLE 3

Inhibition of p51/p66 RT *in vitro* by combinations of TSAOe^{3}T and 9-NH_2N.

Assays were carried out in triplicate with poly (rC)-oligo (dG) and [^{3}H]deoxy-GTP as described in Materials and Methods. In control experiments, the K_m values for deoxy-GTP and poly (rC)-oligo (dG) were determined to be 1 μM and 40 nM, respectively. Combination indices were calculated for mutually nonexclusive inhibitors according to the method of Chou and Talalay (31).

Assay condition	Combination index	
	CI_{50}	CI_{70}
K_m T/P + K_m deoxy-GTP	1.4 ± 0.05	1.2 ± 0.03
0.5 K_m T/P + 5 K_m deoxy-GTP	1.0 ± 0.1	0.8 ± 0.1
5 K_m T/P + 0.5 K_m deoxy-GTP	1.2 ± 0.05	1.0 ± 0.05

TABLE 4

Ability of TSAOe3T to protect HIV-1 RT mechanistic forms from irreversible photoinactivation by 9-AN

RT mechanistic forms were prepared; photoprotection studies of these different RT mechanistic forms were carried out as we have described previously (14). The concentration of the 9-AN photolabel was 1 μM, and that of $TSAOe^3T$, where present, was 12.5 μM. Values are the means ± standard deviation of three separate determinations.

RT mechanistic form	Rate of inactivation	
	− $TSAOe^3T$	+ $TSAOe^3T$
	min^{-1}	
Free RT	0.035 ± 0.002	0.035 ± 0.003
RT-T/P binary complex	0.044 ± 0.004	0.036 ± 0.002
RT-T/P-deoxy-GTP ternary complex	0.036 ± 0.002	0.036 ± 0.002

$TSAOe^3T$ was unable to protect either free RT or the RT-T/P-dNTP ternary complex from photoinactivation by 9-AN (Table 4). Although some apparent photoprotection was noted for the RT-T/P binary complex (Table 4), this was obtained only with very high concentrations of $TSAOe^3T$, well above the apparent IC_{50} value shown in Table 1 for this inhibitor. In contrast, 9-NH_2N completely protected all three RT mechanistic forms from photoinactivation by 9-AN (data not shown).

Effect of inhibitor concentration on RT RDDP product distribution. Although HIV-1 RT DNA polymerase activity is essentially processive, under certain conditions, a number of different length polymerization products can be observed because of transcriptional pausing and/or template-primer dissociation events that occur during reverse transcriptase-catalyzed primer extension (34–37).

The heteropolymeric RDDP template used in these studies corresponds to the sequence of the HXB2D HIV-1 genomic RNA template used for synthesis of viral (−)strong stop DNA (29). With a synthetic 18-nucleotide DNA oligonucleotide as primer and in the absence of inhibitor, a number of polymerization products are seen (Fig. 2A).

$TSAOe^3T$ inhibited the formation of all polymerization products (Fig. 2A, *lanes 2–4*). Although the amount of the full-length (−)strong stop DNA product (n+173) was decreased by $TSAOe^3T$, this decrease was not accompanied by a significant accumulation of smaller polymerization products (Fig. 2B). In contrast, inhibition by 9NH_2N (Fig. 2A, *lanes 6–8*) resulted in a complete loss of full-length product n+173, accompanied by an apparent increase in smaller polymerization products (Fig. 2B).

Time course of RT RDDP activity under continuous and single-cycle processive conditions in the absence and the presence of $TSAOe^3T$ and 9-NH_2N. The apparent differences in the polymerization product distribution profiles in the presence of $TSAOe^3T$ and 9-NH_2N prompted us to further investigate these mechanisms. In these experiments, the concentrations of $TSAOe^3T$ and 9-NH_2N were adjusted to provide approximately 70–75% inhibition. Continuous polymerization (Fig. 3) and single processive cycle (Fig. 4) exper-

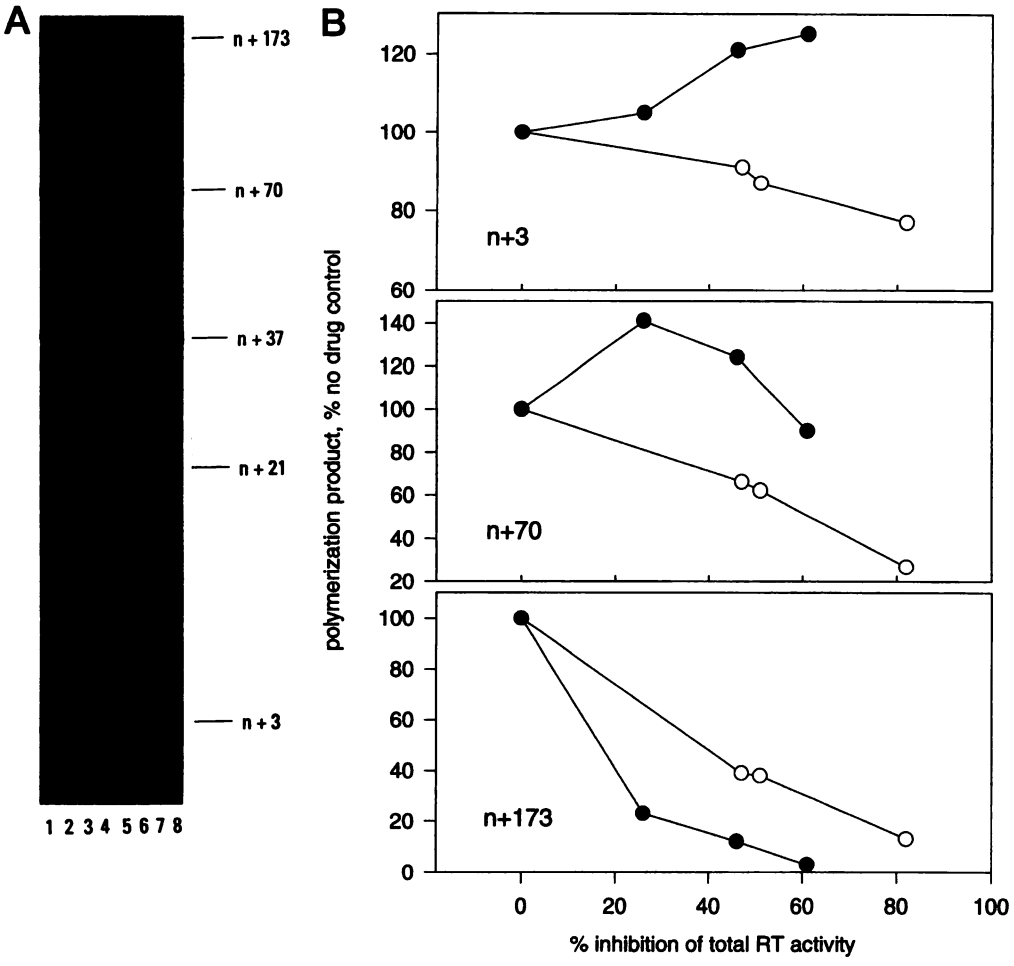

Fig. 2. Effect of inhibitor concentration on RT RDDP product distribution. A, Autoradiogram of polymerization products separated by PAGE. Reactions contained the pHIV-PBS RNA transcript T/P (35.5 nM), RT p51/p66 heterodimer (3.4 nM), and 5 μM each of deoxy-ATP, [α-^{32}P]deoxy-CTP, deoxy-GTP and deoxy-TTP. Reactions were carried out for 10 min. at 37°, then quenched and analyzed by PAGE as described in Materials and Methods. *Lanes 1–4*, $TSAOe^3T$ (0, 3, 6, 12 μM); *lanes 5–8*, 9-NH_2N (0, 0.75, 1.5, 3 μM). Major polymerization products are indicated at n+3, n+21, n+37 and n+70. Full-length product is n+173. B, Graphical representation of the variation of selected polymerization products with increasing inhibition by $TSAOe^3T$ (○) and 9-NH_2N (●). RT RDDP polymerization products from the gel illustrated in Fig. 2A were excised and the radioactivity was determined by liquid scintillation counting.

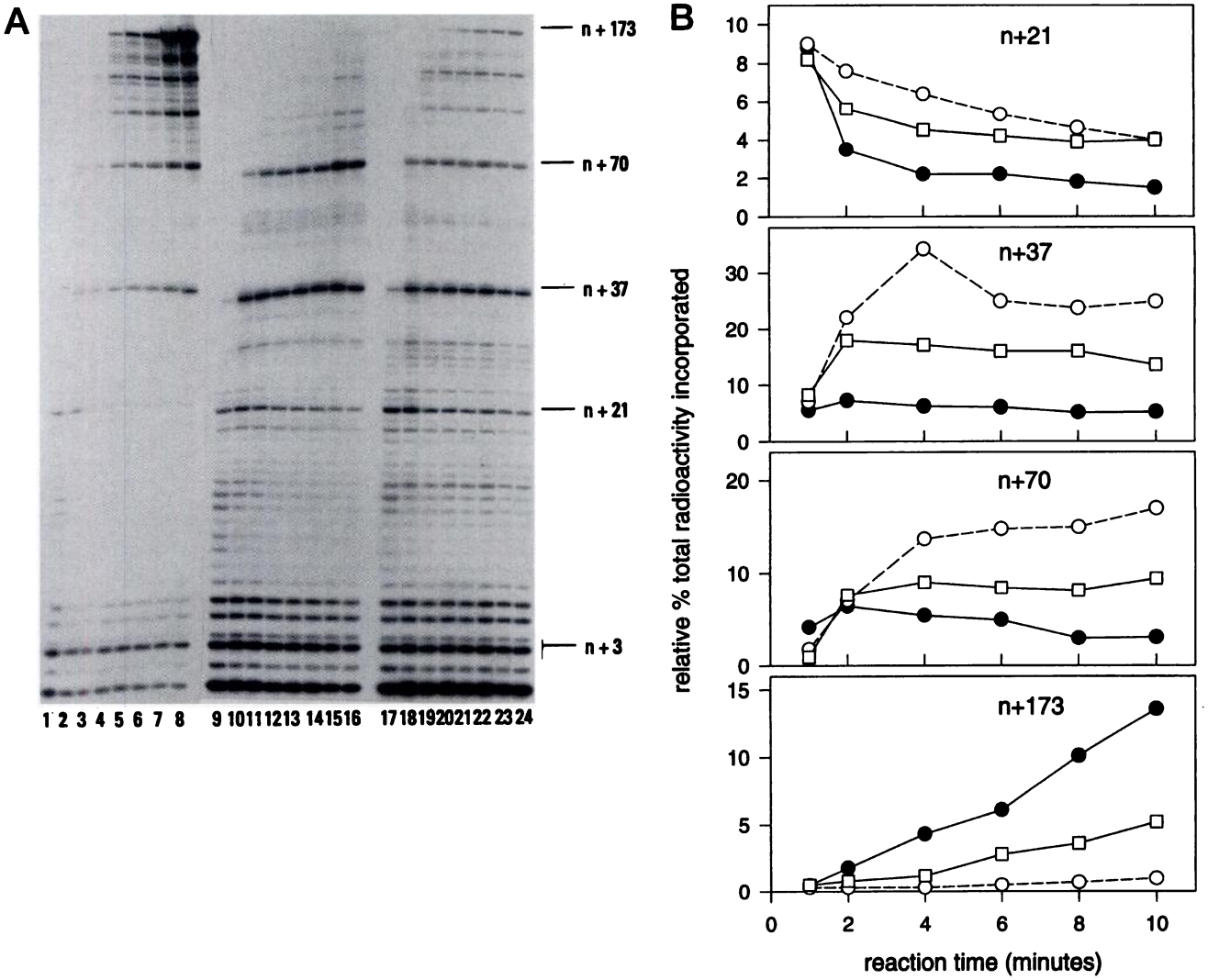

Fig. 3. Time course of polymerization product distribution under continuous assay conditions. A, Autoradiogram of polymerization product profiles in the absence of inhibitor (*lanes 1–8*) or the presence of 4 μM 9-NH_2N (*lanes 9–16*) or 7 μM TSAOe^{3}T (*lanes 17–24*). Reactions were carried out at 37° and contained the pHIV-PBS RNA transcript T/P (74 nM) and RT p51/p66 heterodimer (4.5 nM); they were initiated by the addition of a dNTP mix, which gave a final concentration of 25 μM each of deoxy-ATP, [α-^{32}P]deoxy-CTP, deoxy-GTP, and deoxy-TTP. Samples were removed at 1, 2, 4, 6, 8, 10, 30, and 60 min after the addition of the dNTPs and were quenched and analyzed by PAGE as described in Materials and Methods. B, Graphical representation of the variation of selected polymerization products with time in the absence of inhibitor (●) or in the presence of TSAOe^{3}T (□) or 9-NH_2N (○). RT RDDP polymerization products from the gel illustrated in Fig. 3A were excised and analyzed by liquid scintillation counting.

iments were carried out under similar conditions, except that single-cycle experiments contained heparin as a "trap" after preincubation of RT with the T/P. Heparin competes with the T/P for binding to free RT (32). This allows observation of the polymerization product distribution under conditions of a single processive cycle, because RT, upon dissociation from the T/P, is trapped by the heparin and therefore unable to rebind to the T/P and continue transcription of the partial polymerization products.

In the absence of inhibitor, discernable n+173 full-length product was noted after about 4 min of reaction (Figs. 3 and 4). Similarly, in the presence of TSAOe^{3}T, n+173 full length product was noted after approximately the same time of polymerization, under both continuous and single processive cycle conditions (Figs. 3 and 4), even though overall RT RDDP activity was inhibited by 70% under these conditions. In contrast, with 9-NH_2N under continuous polymerization conditions, the n+173 full length product was discernable only after 30 min of reaction (Fig. 3A). In single processive cycle experiments with 9-NH_2N, no full-length n+173 product was observed even after 60 min of reaction (Fig. 4A).

In the experiments shown in Figs. 3 and 4, significant polymerization pausing was noted after the addition of the first nucleotide, as has been found by others using different templates (37, 38). This has been proposed to result from a higher probability of termination at this site, with the initiation of polymerization and the subsequent elongation representing distinct kinetic phases (39). In our experiments, this strong pause site at n+1 was more apparent in the presence of high concentrations of dNTP. For example, 25 μM dNTP was used in the experiments shown in Figs. 3 and 4, whereas the experiments illustrated in Fig. 2 employed 5 μM dNTP. In the latter case, the n+1 products were significantly diminished.

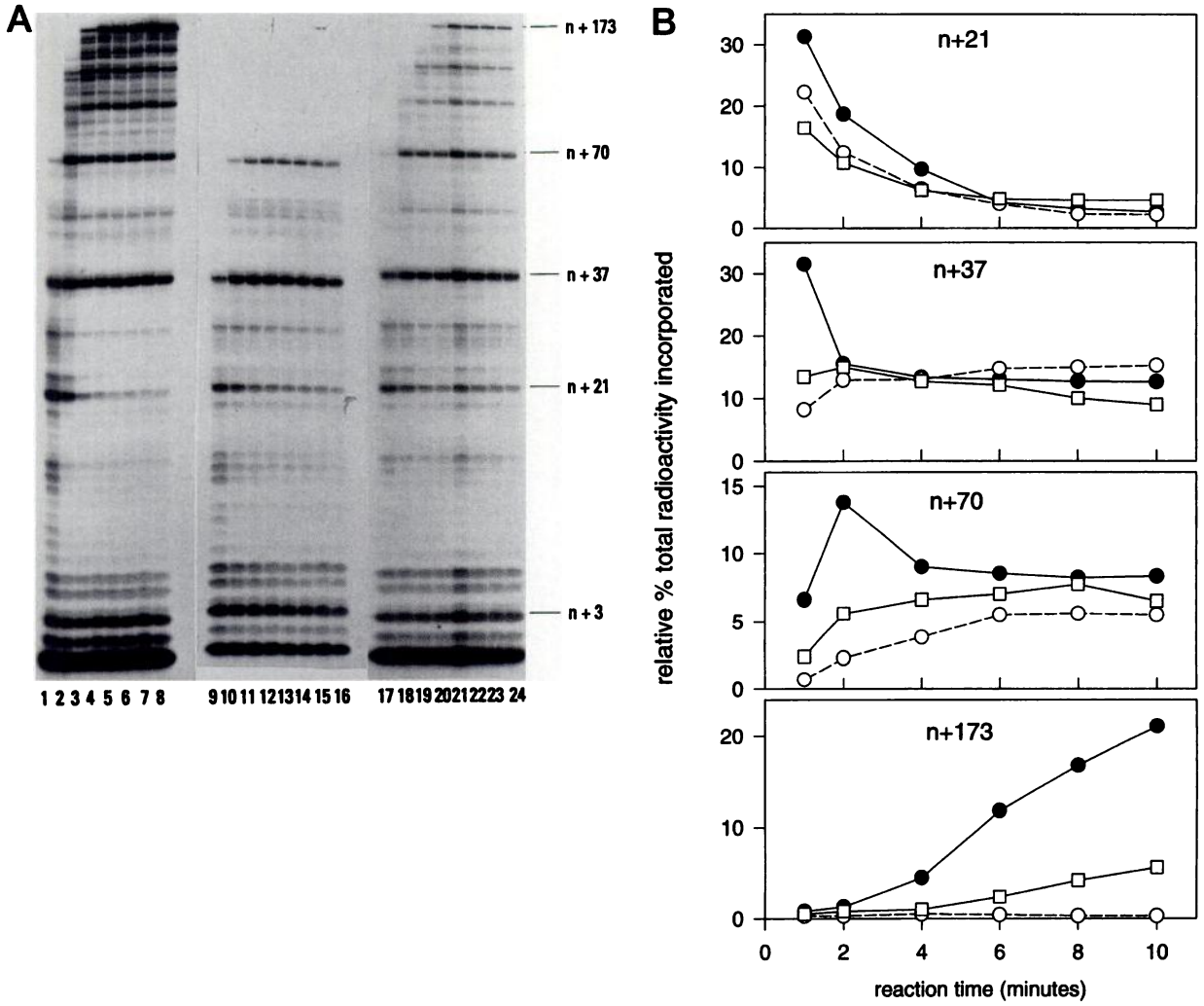

Fig. 4. Time course of polymerization product distribution under single processive cycle conditions. A, Autoradiogram of polymerization product profiles in the absence of inhibitor (*Lanes 1–8*) and in the presence of 4 μM 9-NH_2N (*lanes 9–16*) or 7 μM TSAOe^{3}T (lanes *17–24*). p51/p66 RT (4.5 nM) was preincubated with pHIV-PBS RNA transcript T/P (148 nM) for 3 min at 37°, then reactions were initiated by the simultaneous addition of deoxy-ATP, [α-^{32}P]deoxy-CTP, deoxy-GTP, and deoxy-TTP to a final concentration of 25 μM each and heparin to a final concentration of 1 mg/ml. Samples were removed at 1, 2, 4, 6, 8, 10, 30, and 60 min after the addition of the dNTPs, quenched, and analyzed by PAGE as described in Materials and Methods. B, Graphical representation of the variation of selected polymerization products with time in the absence of inhibitor (●) or in the presence of TSAOe^{3}T (□) or 9-NH_2N (○). RT RDDP polymerization products from the gel illustrated in Fig. 4A were excised and the radioactivity determined by liquid scintillation counting.

Discussion

TSAO inhibitors of HIV-1 RT are highly modified nucleoside derivatives (21, 22) (Fig. 1). However, TSAO-mediated inhibition of viral replication does not require metabolism, and kinetic studies have shown that inhibition of RT RDDP by TSAO analogs is distinct from that of other nucleoside-based inhibitors such as AZT (21). This implies that TSAO functions by binding to a site distinct from that which binds dNTP substrate. In this respect, TSAO mimics the NNRTI compounds, a structurally diverse group of HIV-1 RT DNA polymerase inhibitors. Nevirapine is typical of the NNRTI and binds to a hydrophobic site on the RT p66 subunit that can be defined in part by residues 100, 103, 106, 181, 188, and 190, because resistance to NNRTI is associated with mutations in one or more of these residues (33). Recent crystal analyses have confirmed the identity of the NNRTI site (17–20). Although some mutants that are resistant to NNRTI (e.g., V106A, Y181C, Y188H) are also cross-resistant to TSAO, specific resistance to TSAO correlates with a E138K mutation, which does not confer cross-resistance either to NNRTIs (such as nevirapine) or to dideoxynucleoside antivirals (such as AZT) (23). In addition, in distinct contrast to mutations associated with resistance to NNRTI, resistance to TSAO is attributable to modification of the p51 subunit of RT (24, 25). Nonetheless, the p51 E138 residue is very near to the NNRTI pocket on p66 (33). Thus, although it is conceivable that TSAO may function by interacting with the well-defined NNRTI pocket, this binding is not certain. The experiments described in the present report have attempted to clarify this question.

Both TSAOe^{3}T and 9-NH_2N were equally effective at inhibiting the DNA polymerase activity of the RT p51/p66 heterodimer on a variety of T/P (Table 1), and both function as mixed, noncompetitive inhibitors of the RT p51/p66 heterodimer (data not shown). These observations are consistent with similar mechanisms for binding to RT. However, viral

resistance to nevirapine and TSAO correlates with different mutations in the p66 and p51 subunits of RT, respectively. Our purification protocol provides active p51/p51 and p66/p66 homodimeric forms of RT (30). Although the biological status of these homodimeric forms of RT is uncertain, the homodimers possess significant levels of DNA polymerase activity and can therefore serve as useful mechanistic probes in inhibitor studies. We found that 9-NH_2N was virtually inactive against the DDDP activity of both p51/p51 and p66/p66 homodimeric RT (Table 2), which indicates that the NNRTI binding pocket may be significantly altered in the RT homodimers. In contrast, TSAOe^{3}T was a good inhibitor of the DDDP activity of both p51/p51 and p66/p66 homodimeric RT (Table 2), which indicates that a binding pocket exists for TSAOe^{3}T but not for 9-NH_2N in the RT homodimers and implies different modes of binding to RT for the nevirapine and TSAO analogs.

Several mechanistic species of RT are involved in proviral DNA synthesis. We have previously shown that the efficacy of NNRTI inhibition of RT depends largely on the mechanistic form of RT present in the reaction assay (14, 15). Nevirapine analogs bind to all three mechanistic forms of RT: free RT, RT-T/P binary complex, and the RT-T/P-dNTP ternary complex (14). Crystallographic studies have shown that such NNRTIs as nevirapine, α-anilinophenylacetamide and tetrahydroimidazo[4,5,1-*jk*][1,4]-benzodiazepine-2(1*H*)-thione all bind to the same well-defined site on RT (17–20). Irreversible inactivation of RT by the photolabel 9-AN is prevented by the presence of other NNRTI, such as nevirapine (27), and the carboxanilides (14). In the present studies, we found that 9-NH_2N was able to photoprotect all RT mechanistic forms (data not shown), which implies that 9-NH_2N competes for the same site on RT as nevirapine. In contrast, TSAOe^{3}T was unable to significantly protect any of these mechanistic forms of RT from inactivation by the nevirapine analog photoaffinity label 9-AN (Table 3), even when present at a concentration nearly 20-fold higher than its IC_{50} value and in 10-fold excess over that of the 9-AN photolabel. It therefore seems that TSAOe^{3}T interacts with RT in a manner very different than nevirapine.

Further evidence for the differential binding of TSAOe^{3}T and 9-NH_2N was obtained from our studies of the RDDP polymerization product distributions obtained under continuous and single processive cycle conditions. In the absence of inhibitor, several polymerization products are evident (Figs. 2A, 3A, 4A). Transcriptional pausing occurs at homopolymeric nucleotide stretches as well as at regions of nucleic acid secondary structure (37). Two of the polymerization products in our experiments (n+37, n+70) correspond to regions of three consecutive cytidylic acid residues. The product at n+3 may result from pausing caused by a RNA hairpin secondary structure at this point.[1] The n+173 product is the full-length DNA.

The experiments carried out under single processive cycle conditions (Fig. 4) show that the various products arise via two distinct polymerization termination mechanisms (37). The first is polymerization stalling, in which RT remains bound to the T/P with the possibility of further product elongation. The second is RT dissociation from the T/P. In this case, no further product extension is possible because the presence of the heparin "trap" prevents rebinding of RT to the T/P. In the former case, the intensity of the polymerization product will decrease with time because of subsequent reinitiation of polymerization with the stalled RT-T/P complex. However, polymerization products created by T/P dissociation will remain relatively constant or increase with the time of reaction.

The polymerization products at n+1, n+3, n+37 and n+70 correspond to dissociation events, whereas that at n+21 is consistent with polymerization stalling. Under continuous polymerization conditions (Fig. 3), both TSAOe^{3}T and 9-NH_2N have similar effects on the n+21 product, increasing polymerization stalling at this site. However, 9-NH_2N seems to be more effective than TSAOe^{3}T in promoting the dissociation events that lead to products at n+37 and n+70 (Fig. 3B). The most striking difference between inhibition by TSAOe^{3}T and 9-NH_2N is the absence of n+173 full-length product in the presence of the latter inhibitor under both continuous and single processive cycle conditions.

Thus, although TSAOe^{3}T and 9-NH_2N may be equally effective at reducing the overall rate of RT polymerase activity, the inhibitors seem to function by different mechanisms. TSAOe^{3}T does not substantially alter the polymerization product profile, because all products noted in the absence of inhibitor, including n+173 full length product, are evident in the TSAOe^{3}T-inhibited reactions. In contrast, 9-NH_2N effectively prevents the formation of full length product, despite the lack of a commensurate decrease in shorter length products. Interestingly, the pyridinone inhibitor L-697,661 (which binds to the same NNRTI site as nevirapine) also promotes the appearance of polymerization products that are shorter than full length (40).

In conclusion, our data, when considered with previously published information on the mechanism of NNRTI inhibition of RT, implies that TSAOe^{3}T may inhibit HIV-1 RT either by interacting with the NNRTI site differently than other NNRTI or by binding to a site somewhat distinct from the sites of NNRTI or dNTP binding. Preliminary molecular modeling studies[2] are consistent with the idea that TSAOe^{3}T may bind to a region of RT close to and partially overlapping with the the well-defined NNRTI binding pocket. However, confirmation of this conjecture must of course await crystallographic analysis of the RT-TSAOe^{3}T adduct.

References

1. Mitsuya, H., K. J. Weinhold, P. A. Furman, M. H. St. Clair, S. N. Lehrman, R. C. Gallo, D. Bolognesi, D. W. Barry, and S. Broder. 3′-Azido-3′deoxythymidine (BWA509U): an antiviral agent that inhibits the infectivity and cytopathic effect of human T-lymphotropic virus type III/lymphadenopathy-associated virus *in vitro*. *Proc. Natl. Acad. Sci. USA* **82**:7096–7100 (1985).
2. Yarchoan, R., H. Mitsuya, R. V. Thomas, J. M. Pluda, N. R. Hartman, C-F. Perno, K. S. Marczyk, J-P. Allain, D. G. Johns, and S. Broder. In vitro activity against HIV and favorable toxicity profile of 2′3′-dideoxyinosine. *Science (Washington D. C.)* **245**:412–415 (1989).
3. Huang, P., D. Farquhar, and W. Plunkett. Selective action of 3′-azido-3′-dideoxythymidine 5′-triphosphate on viral reverse transcriptase and human DNA polymerases. *J. Biol. Chem.* **265**:11914–11918 (1990).
4. Soudeyns, H., X-J. Yao, Q. Gao, B. Belleau, J-L. Kraus, N. Nguyen-Ba, B. Spira, and M. A. Wainberg. Anti-human immunodeficiency virus type 1 activity and in vitro toxicity of 2′-deoxy-3′-thiacytidine (BCH-189), a novel heterocyclic nucleoside analog. *Antimicrob. Agents Chemother.* **35**:1386–1390 (1991).
5. Schinazi, R. F., C. K. Chu, A. Peck, A. McMillan, R. Mathis, D. Cannon, L-S. Jeong, J. W. Beach, W-B. Choi, S. Yeola, and D. C. Liotta. Activities of

[1] D. Arion and M. A. Parniak, unpublished observations.

[2] G. I. Dmitrienko, N. J. Taylor, J. Balzarini, M.-J. Camarasa and M. A. Parniak, unpublished observations.

the four optical isomers of 2′,3′-dideoxy-3′-thiacytidine (BCH-189) against human immunodeficiency virus type 1 in human lymphocytes. *Antimicrob. Agents Chemother.* **36**:672–676 (1992).
6. Furman, P. A., J. A. Fyfe, M. H. St. Clair, K. Weinhold, J. L. Rideout, G. A. Freeman, S. N. Lehrman, D. P. Bolognesi, S. Broder, H. Mitsuya, and D. W. Barry. Mode of inhibition of the human T-cell lymphotropic virus III by 3′-azido-3′-dideoxythymidine. *Proc. Natl. Acad. Sci. USA* **83**:8333–8337 (1986).
7. Gu, Z., R. S. Fletcher, E. J. Arts, M. A. Wainberg, and M. A. Parniak. The K65R mutant reverse transcriptase of HIV-1 cross resistant to 2′,3′-dideoxycytidine, 2′,3′-dideoxy-3′-thiacytidine, and 2′,3′-dideoxyinosine shows reduced sensitivity to specific dideoxynucleoside triphosphate inhibitors *in vitro*. *J. Biol. Chem.* **269**:28118–28122 (1994).
8. Gu, Z., E. J. Arts, M. A. Parniak, and M. A. Wainberg. Mutated K65R recombinant reverse transcriptase of human immunodeficiency virus type 1 shows diminished chain termination in the presence of 2′,3′-dideoxycytidine 5′-triphosphate and other drugs. *Proc. Natl. Acad. Sci. USA* **92**:2760–2764 (1995).
9. Merluzzi, V. J., K. D. Hargrave, M. Labadia, K. Grozinger, M. T. Skoog, J. C. Wu, C-K. Shih, K. Eckner, S. Hattox, J. Adams, A. S. Rosehthal, R. Faanes, R. J. Eckner, R. A. Koup, and J. L. Sullivan. Inhibition of HIV-1 replication by a nonnucleoside reverse transcriptase inhibitor. *Science (Washington D. C.)* **250**:1411–1413 (1990).
10. Kopp, E. B., J. J. Miglietta, A. G. Shrutkowski, C-K. Shih, P. M. Grob, and M. T. Skoog. Steady state kinetics and inhibition of HIV-1 reverse transcriptase by a non-nucleoside dipyridodiazepinone, BI-RG-587, using a heteropolymeric template. *Nucleic Acids Res.* **19**:3035–3039 (1991).
11. Pauwels, R., K. Andries, J. Desmyter, D. Schols, M. J. Kukla, H. J. Breslin, A. Raeymaeckers, J. Van Gelder, R. Woestenborghs, J. Heykants, K. Schellekens, M. A. Janssen, E. De Clercq, and P. A. J. Janssen. Potent and selective inhibition of HIV-1 replication in vitro by a novel series of TIBO derivatives. *Nature (Lond.)* **343**:470–474 (1990).
12. Goldman, M. E., J. H. Nunberg, J. A. O'Brien, J. C. Quintero, J. M. Schlief, K. F. Freund, S. L. Gaul, W. S. Saari, J. S. Wai, J. M. Hoffman, P. S. Anderson, D. J. Hupe, E. A. Emini, and A. M. Stern. Pyridone derivatives: specific human immunodeficiency virus type 1 reverse transcriptase inhibitors with antiviral activity. *Proc. Natl. Acad. Sci. USA* **88**:6863–6867 (1991).
13. Bader, J. P., J. B. McMahon, R. J. Schultz, V. L. Narayanan, J. B. Pierce, O. S. Weislow, C. F. Midelfort, S. F. Stinson, and M. R. Boyd. Oxathiin carboxanilide, a potent inhibitor of human immunodeficiency virus reproduction. *Proc. Natl. Acad. Sci. USA* **88**:6740–6744 (1991).
14. Fletcher, R. S., K. Syed, S. Mithani, G. I. Dmitrienko, and M. A. Parniak. Carboxanilide derivative non-nucleoside inhibitors of HIV-1 reverse transcriptase interact with different mechanistic forms of the enzyme. *Biochemistry* **34**:4346–4353 (1995).
15. Fletcher, R. S., D. Arion, G. Borkow, M. A. Wainberg, G. I. Dmitrienko, and M. A. Parniak. Synergistic inhibition of HIV-1 reverse transcriptase DNA polymerase activity and virus replication *in vitro* by combinations of carboxanilide nonnucleoside compounds. *Biochemistry* **34**:10106–10112 (1995).
16. Wu, J. C., T. C. Warren, J. Adams, J. Proudfoot, J. Skiles, P. Raghavan, C. Perry, I. Potocki, P. R. Farina, and P. M. Grob. A novel dipyridodiazepinone inhibitor of HIV-1 reverse transcriptase acts through a nonsubstrate binding site. *Biochemistry* **30**:2022–2026 (1991).
17. Kohlstaedt, L. A., J. Wang, J. M. Friedman, P. A. Rice, and T. A. Steitz. Crystal structure at 3.5 A resolution of HIV-1 reverse transcriptase complexed with an inhibitor. *Science (Washington D. C.)* **256**:1783–1790 (1992).
18. Smerdon, S. J., J. Jäger, L. A. Kohlstaedt, A. J. Chirino, J. M. Friedman, P. A. Rice, and T. A. Steitz. Structure of the binding site for nonnucleoside inhibitors of the reverse transcriptase of human immunodeficiency virus type 1. *Proc. Natl. Acad. Sci. USA* **91**:3911–3915 (1994).
19. Ding, J., K. Das, H. Moereels, L. Koymans, K. Andries, P. A. J. Janssen, S. H. Hughes, and E. Arnold. Structure of HIV-1 RT/TIBO R 86183 complex reveals similarity in the binding of diverse nonnucleoside inhibitors. *Nat. Struct. Biol.* **2**:407–415 (1995).
20. Ren, J., R. Esnouf, E. Garman, D. Somers, C. Ross, I. Kirby, J. Keeling, G. Darby, Y. Jones, D. Stuart, and D. Stammers. The structure of HIV-1 reverse transcriptase complexed with 9-chloro-TIBO: lessons for inhibitor design. *Nat. Struct. Biol.* **2**:293–302 (1995).
21. Balzarini, J., M-J. Pérez-Pérez, A. San-Félix, M-J. Camarasa, I. C. Bathurst, P. J. Barr, and E. De Clercq. Kinetics of inhibition of human immunodeficiency virus type 1 (HIV-1) reverse transcriptase by the novel HIV-1-specific nucleoside analogue [2′,5′-bis-*o*-(*tert*-butyldimethylsilyl)-b-D-ribofuranosyl]-3′-spiro-5″-(4″-amino-1″, 2″-oxathiole-2″, 2″-dioxide)thymine (TSAO-T). *J. Biol. Chem.* **267**:11831–11838 (1992).
22. Balzarini, J., M-J. Pérez-Pérez, A. San-Félix, D. Schols, C-F. Perno, A-M. Vandamme, M-J. Camarasa, and E. De Clercq. 2′,5′-bis-*o*-(*tert*-butyldimethylsilyl)-3′-spiro-5″-(4″-amino-1″, 2″-oxathiole-2″, 2″-dioxide) pyrimidine (TSAO) nucleoside analogues: highly selective inhibitors of human immunodeficiency virus type 1 that are targeted at the viral reverse transcriptase. *Proc. Natl. Acad. Sci. USA* **89**:4392–4396 (1992).
23. Balzarini, J., A. Karlsson, A-M. Vandamme, M-J. Pérez-Pérez, H. Zhang, L. Vrang, B. Oberg, K. Backbro, T. Unge, A. San-Felix, S. Velázquez, M-J. Camarasa, and E. De Clercq. Human immunodeficiency virus type 1 (HIV-1) strains selected for resistance against the HIV-1-specific [2′,5′-bis-*o*-(*tert*-butyldimethylsilyl)ribofuranosyl]-3′-spiro-5″-(4″- amino-1″, 2″-oxathiole-2″, 2″-dioxide)]-b-D- pentofuranosyl (TSAO) nucleoside analogues retain sensitivity to HIV-1-specific nonnucleoside inhibitors. *Proc. Natl. Acad. Sci. USA* **90**:6952–6956 (1993).
24. Boyer, P. L., J. Ding. E. Arnold, and S. H. Hughes. Subunit specificity of mutations that confer resistance to nonnucleoside inhibitors in human immunodeficiency virus type 1 reverse transcriptase. *Antimicrob. Agents Chemother.* **38**:1909–1914 (1994).
25. Jonckheere, H., J-M. Taymans, J. Balzarini, S. Velázquez, M-J. Camarasa, J. Desmyter, E. De Clercq, and J. Anné. Resistance of HIV-1 reverse transcriptase against [2′,5′-bis-*o*-(*tert*-butyldimethylsilyl)-3′-spiro-5″-(4″-amino-1″, 2″-oxathiole-2″, 2″-dioxide)] (TSAO). *J. Biol. Chem.* **269**:25255–25258 (1994).
26. Hargrave, K. D., J. R. Proudfoot, K. G. Grozinger, E. Cullen, S. R. Kapadia, U. R. Patel, V. U. Fuchs, S. C. Maudlin, J. Vitous, M. L. Behnke, J. M. Klunder, K. Pal, J. W. Skiles, D. W. McNeil, J. M. Rose, G. C. Chow, M. T. Skoog, J. C. Wu, G. Schmidt, W. W. Engel, W. G. Eberlein, T. D. Saboe, S. J. Campbell, A. S. Rosenthal, and J. Adams. Novel non-nucleoside inhibitors of HIV-1 reverse transcriptase. 1. Tricyclic pyridobenzo- and dipyridobenzodiazepinones. *J. Med. Chem.* **34**:2231–2241 (1991).
27. Grob, P. M., J. C. Wu, K. A. Cohen, R. H. Ingraham, C-K. Shih, K. D. Hargrave, T. L. McTague, and V. J. Merluzzi. Nonnucleoside inhibitors of HIV-1 reverse transcriptase: nevirapine as a prototype drug. *AIDS Res. Hum. Retroviruses* **8**:145–152 (1992).
28. Pérez-Pérez, M-J., A. San-Félix, J. Balzarini, E. De Clercq, and M-J. Camarasa. TSAO analogues. Stereospecific synthesis and anti-HIV-1 activity of [1-[2′,5′-bis-*o*-(tert-butyldimethylsilyl)-b-D-ribofuranosyl]-3′-spiro-5″-(4″-amino-1″, 2″-oxathiole-2″, 2″-dioxide) pyrimidine and pyrimidine-modified nucleosides. *J. Med. Chem.* **35**:2988–2995 (1992).
29. Arts. E. J., X. Li, Z. Gu, L. Kleiman, M. A. Parniak, and M. A. Wainberg. Comparison of deoxyoligonucleotide and $tRNA^{Lys-3}$ as primers in an endogenous human immunodeficiency virus-1 *in vitro* reverse transcription/template switching reaction. *J. Biol. Chem.* **269**:14672–14680 (1994).
30. Fletcher, R. S., G. Holleschak, E. Nagy, D. Arion, G. Borkow, Z. Gu, M. A. Wainberg, and M. A. Parniak. Single-step purification of recombinant wild type and mutant HIV-1 reverse transcriptase. *Protein Expr. Purif.* **7**:27–32 (1996).
31. Chou, T.-C., and P. Talalay. Quantitative analysis of dose-effect relationships: the combined effects of multiple drugs or enzyme inhibitors. *Adv. Enzyme Regul.* **22**:27–55 (1984).
32. Beard, W. A., and S. H. Wilson. Kinetic analysis of template-primer interactions with recombinant forms of HIV-1 reverse transcriptase. *Biochemistry* **32**:9745–9753 (1993).
33. Tantillo, C., J. Ding, A. Jacobo-Molina, R. G. Nanni, P. L. Boyer, S. H. Hughes, R. Pauwels, K. Andries, P. A. J. Janssen, and E. Arnold. Locations of anti-AIDS drug binding sites and resistance mutations in the three-dimensional structure of HIV-1 reverse transcriptase. Implications for mechanism of drug inhibition and resistance. *J. Mol. Biol.* **243**:369–387 (1994).
34. Huber, E. H., J. M. McCoy, J. S. Seerah, and C. C. Richardson. Human immunodeficiency virus 1 reverse transcriptase. Template binding, processivity, strand displacement synthesis, and template switching. *J. Biol. Chem.* **264**:4669–4678 (1989).
35. Williams, K. J., L. A. Loeb, and M. Fry. Synthesis of DNA by human immunodeficiency virus reverse transcriptase is preferentially blocked at template oligo(deoxyadenosine) tracts. *J. Biol. Chem.* **265**:18682–18689 (1990).
36. Abbotts, J., K. Bebenek, T. A. Kunkel, and S. H. Wilson. Mechanism of HIV-1 reverse transcriptase. Termination of processive synthesis on a natural DNA template is influenced by the sequence of the template-primer stem. *J. Biol. Chem.* **268**:10312–10323 (1993).
37. Klarmann, G. J., C. A. Schauber, and B. D. Preston. Template-directed pausing of DNA synthesis by HIV-1 reverse transcriptase during polymerization of HIV-1 sequences *in vitro*. *J. Biol. Chem.* **268**:9793–9802 (1993).
38. Reardon, J. E., E. S. Furfine, and N. Cheng. Human immunodeficiency virus reverse transcriptase. Effect of primer length on template-primer binding. *J. Biol. Chem.* **266**:14128–14134 (1991).
39. Kati, W. M., K. A. Johnson, L. F. Jerva, and K. S. Anderson. Mechanism and fidelity of HIV reverse transcriptase. *J. Biol. Chem.* **267**:25988–25997 (1992).
40. Olsen, D. B., S. S. Carroll, J. C. Culberson, J. A. Shafer, and L. C. Kuo. Effect of template secondary structure on the inhibition of HIV-1 reverse transcriptase by a pyridinone non-nucleoside inhibitor. *Nucleic Acids Res.* **22**:1437–1443 (1994).

Send reprint requests to: Dr. Michael A. Parniak, Lady Davis Institute for Medical Research, 3755 Cote Ste Catherine Road, Montreal, Quebec H3T 1E2, Canada. Email: mparniak@ldi.jgh.mcgill.ca